SEMARAK ILMU PUBLISHING

Journal of Advanced Research in Micro and Nano Engineering

Journal homepage:
https://semarakilmu.com.my/journals/index.php/micro_nano_engineering/index
ISSN: 2756-8210

Electrospray Dynamics: Investigating the Impact of Voltage and Ionization Ring Parameters on Taylor Cone Characteristics

Nurfadzilah Mohd Sani[1], Abdul Rafeq Saleman[1,2,*], Fudhail Abdul Munir[3], Muhammad Hasrul Rosli[3], Ridhwan Jumaidin[4], Mohd Shukri Yob[1], Herman Saputro[5]

[1] Faculty of Technology and Mechanical Engineering, Universiti Teknikal Malaysia Melaka (UTeM), 76100 Durian Tunggal Melaka, Malaysia
[2] Centre for Advanced Research on Energy (CARe), Universiti Teknikal Malaysia, Melaka (UTeM), 76100, Durian Tunggal, Melaka, Malaysia
[3] Department of Mechanical Engineering, Faculty of Engineering, Universiti Teknologi PETRONAS, 32610 Seri Iskandar, Perak, Malaysia
[4] Faculty of Industrial and Manufacturing Technology and Engineering, Universiti Teknikal Malaysia Melaka (UTeM), 76100 Durian Tunggal Melaka, Malaysia
[5] Department of Mechanical Engineering Education, Universitas Sebelas Maret, Surakarta Indonesia

ARTICLE INFO

Article history:
Received 29 July 2024
Received in revised form 2 September 2024
Accepted 15 October 2024
Available online 30 November 2024

Keywords:
Electrospray; droplet; Taylor cone; ring ionization

ABSTRACT

Electrospray is a method used to create droplets from a liquid sample by providing a strong electric field, which are formed by splitting the liquid droplet into charged droplets. The characteristics of the electrospray are influenced by voltage, distance and inner diameter of ionization ring (IDIR). Thus, this paper focuses on the effects of range of voltage, ranges of inner diameter of ionization ring (IDIR) and position of ionization ring (IR). The electrospray was generated by a high voltage generator and syringe pump. By varying the output voltage within 4kV to 10kV, IDIR (10.3 mm, 15.3 mm and 21.2 mm) and distance of 5mm needle to the IR, the generation of Taylor cone were explored. Then, a digital microscope camera was used to capture the phenomenon. The results were evaluated based on the angle generated by the Taylor cone. The results show that the Taylor cone starts to develop at the voltage of 4 kV regardless of the position and IDIR. And at certain voltage the angle of the Taylor cone starts to become constant. This paper offers an initial understanding of the electrospray characters that has potential for vast applications. However, further analysis and experimentation on the factors that affect the character of Taylor cone is needed in optimizing this technique.

1. Introduction

Electrospray technology, which is differentiated by its ability to regulate droplet characteristics through precise electric field applications, is critical in a wide range of commercial and research applications. Due to its capacity to produce liquid or solid aerosol particles by evaporating bulk liquids, electrospray is widely used in a variety of industries, including multiarticulate drug delivery [1], food processing [2], plant nutrition [3], surface coatings [4,5] and many more [6-8]. In brief the concept of electrospray was define as an electro-hydrodynamic (EHD) atomization process that

* *Corresponding author.*
E-mail address: rafeq@utem.edu.my

https://doi.org/10.37934/armne.25.1.5265

utilized an electric field to turn liquid droplets into Taylor cone, overcoming surface tension of the liquid (medium) by electrostatic forces [9]. A strong electric field is applied to the tip of a capillary or nozzle [10], causing a thin jet to emerge which is widely known as Taylor cone. This jet is continuously fragmented into smaller droplets, providing substantial flexibility in altering droplet size and charge composition during the electrospray process [11].

William Gilbert, the first to see and document the effects of an electric field on a liquid surface, made significant contributions to EHD. His main work, "The Magnete," published in 1600, gave crucial insights into how electric fields influence the behavior of liquid droplets. Gilbert's pioneering discoveries established the framework for further research on electrospray phenomena [12]. In 2005, Yeo *et al*., [13] conducted a rigorous examination of the impacts of electric fields on droplet size, distribution, and charge, shedding light on the complex link between electric fields and droplet characteristics. Furthermore, on 2017, Ondimu *et al.,* [14] conducted a comprehensive study that corroborated and built on Gilbert's findings, underlining its long-term importance in current electrospray research. Their discoveries highlighted the dynamic nature of electrospray events and their numerous applications. The behavior of droplets during electrospraying changes based on the properties of the applied electric field, resulting in different electrospray modes [15].

The electrospray system allows for easy control over droplet size and movement by manipulating the external environment [11,16]. Its construction is simpler than other spray systems and may be customized based on voltage. Droplets repel each other when sprayed into an electric field between a nozzle and a substrate [17], as they are charged with negative (-) ions on their surface [18]. As a result, droplets seldom combine or polymerize [18]. Compared to conventional spray systems, this method produces homogenous and small droplets with minimum dispersion due to their charged properties [19,20]. The voltage applied has a noticeable effect on the production and behavior of the Taylor cone [21]. It controls the strength of the electric field, which influences the creation of the Taylor cone and subsequent jets [22]. Lower voltages produce bigger liquid droplets because the electric force may be insufficient to maintain a continuous jet formation [23]. As the voltage increases, the jet becomes steadier and produces smaller, more uniform droplets. Another crucial component is the ionization ring (IR), which influences spatial distribution and droplet size [24]. The position and size of the IR can have a substantial impact on the electric field distribution surrounding the jet, impacting Taylor cone breakage and creation [25].

Hartman *et al*., [26] provide the physical numerical model that properly calculates the geometry of the liquid cone and jet, as well as the current and surface charge distribution. Electrohydrodynamic atomization in the cone-jet mode produces a size distribution that varies based on the jet's diameter and droplet formation [27]. A stable cone-jet mode requires a minimum flow rate for each liquid. At this minimal flow rate, the jet breaks apart due to axisymmetric instabilities which are also known as varicose instabilities [28]. Higher flow rates result in increased current through the liquid cone [29]. As the current increases, so does the jet's surface charge. Jet break-up above a particular surface charge and can be affected by lateral or azimuthal instabilities. These instabilities are also known as kink instabilities. When the effect of these kink instabilities rises, the size distribution of major droplets widens [30].

Fundamentally, to creates Taylor Cone, a high voltage potential is applied to the liquid either directly to the feeding capillary or to an immersed electrode in relation to a grounded electrode located downstream [12]. An electric field forms around the liquid drop pouring from the capillary tube, causing it to deform into a cone-like shape and discharge a jet from its vertex [31]. A steady state occurs when the flow rate from the capillary needle to the conical meniscus equals that of the jet [32]. The careful handling of many parameters is critical for optimizing the electrospray process in diverse applications [33]. This precise control over droplet generation yields more consistent and

reproducible results, which is critical for sensitive equipment [34]. Furthermore, recent studies have looked at the innovative usage of electrospray-generated jets for micropower production. This includes converting the kinetic energy of Taylor cones into electrical energy, providing a novel technique of energy collecting [35]. Thus, based on past studies that highlight the influences of the parameters, it is understood that a clear insight on the electrospray parameters to generate the Taylor cone is crucial for future study.

Several investigations have been done on electrospray in the past, that utilizes cold spray ionization highlight by Yamaguchi [36], sub-ambient pressure develop by Huang *et al.,* [37] and Ouyang and Cooks [38], in field nano-electrospray ionization has been conducted by Zhong et *al.,* [39] and many more [32,33,40,41]. To the best of the author's knowledge, the Taylor cone is determined based on factors such as size, diameter and position of the IR. However, based on past investigations it is found that clearly insight on these parameters especially the position and dimension of the IR that help in determining the best Taylor cone is less numerous. As understood from literature, understanding and optimizing of these variables are crucial for maximizing the effectiveness of electrospray in diverse applications. Thus, in this paper the distance of the ring ionization, diameter and positioning of the IR will be investigated to give clear insight of the factors that largely influence the Taylor cone behaviors.

2. Methodology

2.1 Material and Setup

A schematic depiction of the experimental apparatus is shown in Figure 1. A high voltage power supply 71030 Series, DC electric field generated 0 to 10 kV output with output current 3.0 mA which was developed by Genvolt. Set the voltage output to the desired level (typically between 4 kV to 10 kV for electrospray production) using the control interface provided. Prepare the syringe pump (NE-1000 series) used to control flow rates of liquid by loading the desired solution into a 60 mL syringe that has an inside diameter of 29.7 mm with infusion maximum rates of 35.33 mL/min. This syringe pump operated from a 12 VDC power supply. Standard needle (model FU-3-6 Tomix) with an appropriate gauge 20 G with outer diameter 0.88 mm and inner diameter 0.55 mm and needle length tip 80 mm was connect to the output of the syringe. Position the IR downstream from the needle tip at a suitable distance to facilitate droplet desolation and ionization. The ring is connected to the electrode to the ground of the power supply to establish the necessary electric field.

Turn on the power supply and set the voltage to the predetermined value required for electrospray ionization (4 kV-10 kV). Initiate the syringe pump to start delivering the solution at a controlled flow rate of 0.10 mL/min through the electrospray needle. Throughout the study, the flow rate of the solution through the electrospray needle was maintained at a constant rate which is 0.1 mL/min. However, adjustments were made to both the power supply settings, the position and dimension of the ionization ring. The dimensions of the ionization ring are the inner diameter of the ionization ring (IDIR) which are set at approximately 10.3 mm, 15.3 mm and 21.2 mm. The thickness of the IR is constant at 1.9 mm. These modifications were undertaken to evaluate their impact on the stability and formation of the Taylor cones.

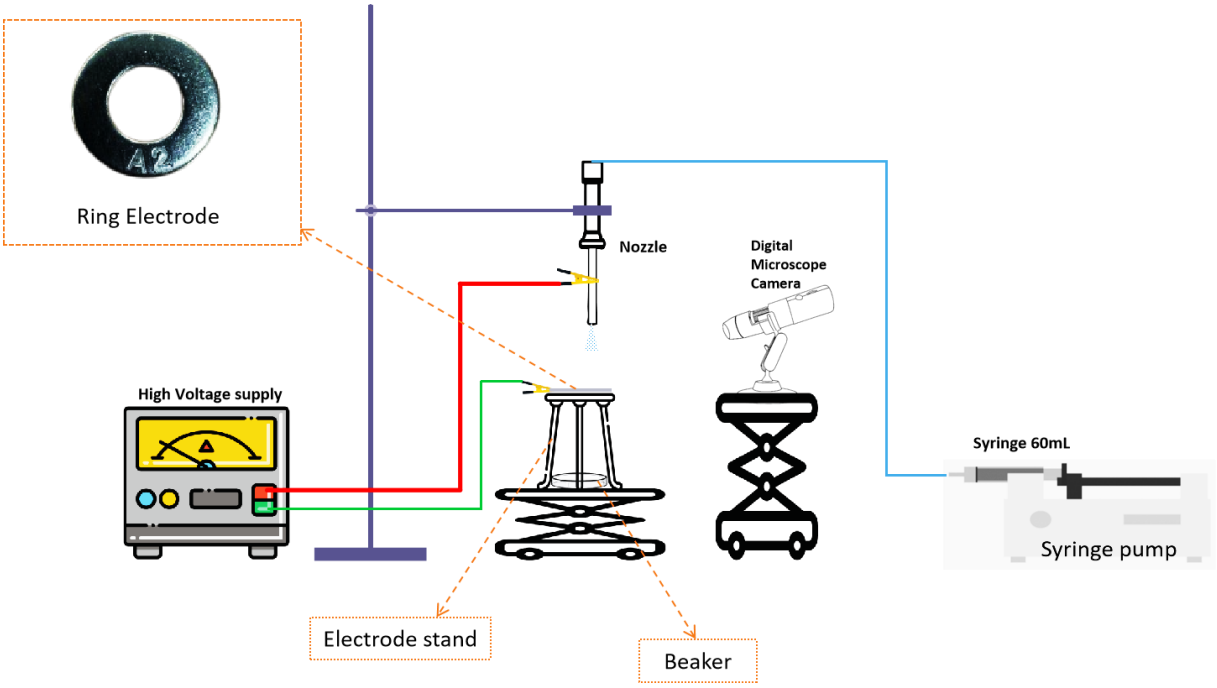

Fig. 1. Schematic of the experimental setup

Another parameter concern in this investigation is the position of the needle. A schematic of positioning the needle tip relation to IR is shown in Figure 2. Position A setup is the tip of the needle above the IR and position B, the needle tip is placed passes IR. This setup is to determine the voltage level that will sustain the stability and endurance of the Taylor cones. The IDIR is also considered since it contributes to the formation of stable Taylor cones.

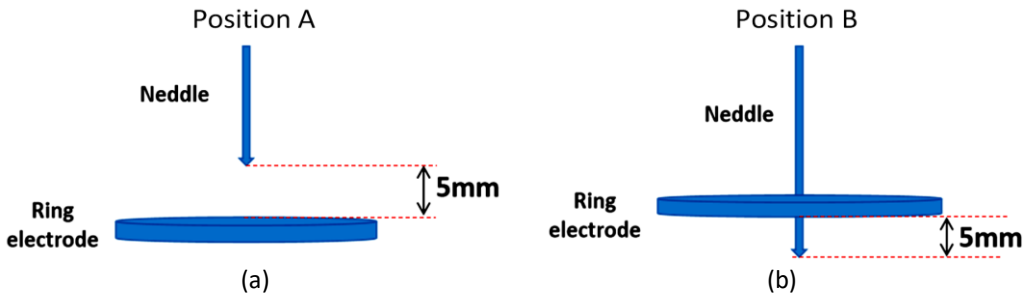

Fig. 2. Schematic positioning needle tip to ionization ring (a) Position A: above ionization ring (b) Position B: passes ionization ring

2.2 Digital Microscope Camera Setup

The U500X model digital microscope camera is utilized to capture the generation of Taylor cone. The microscope camera has a video capture resolution of 0.3 Megapixel and image capture resolution of 640 x 480 pixels per inch. They accompany sensors of substantial resolution in such cameras, which can portray the movement of the Taylor cone and generation of the electrospray. moreover. The camera has a focus range of 15 mm to 40 mm, thus, the shape of beads or the size of the spread, can be recorded clearly. Additionally, with a Frame rate of 30 frame per second under 600 illuminance (LUX) brightness refers to how many times the image is flashed on the screen during a certain second to give the illusion of real movement. However, it should concentrate on points akin to the specific area where the Taylor cone appears and the electrospray needle. Tracing its progression becomes

simple as the camera records delayed pictures and films under numerous experimental conditions. To assure exactness in assessment and imaging, a meticulously detailed positioning and calibration procedure is needed before the commencement of the trial for organizing the camera. The alignment procedure, ensuring the optimal data accumulation, requires having the cardinal position of the electrospray needle as well as the zone apparent in the camera's field of view.

2.3 Data Collection and Analysis

In the field of electrospray experiment, the angle of Taylor cones plays a crucial role in determining the effectiveness of the process. In this experiment, the reliable computer-aided design and drafting programme AutoCAD will be used to record and examine the Taylor cone angles produced by experimental setup. The electrospray Taylor cones are first capture using a digital microscope camera. After they are taken, these pictures must be imported into the AutoCAD programme. The comprehensive measuring and annotation capabilities in AutoCAD are then used to enable a thorough examination of the bead angles shown in Figure 3.

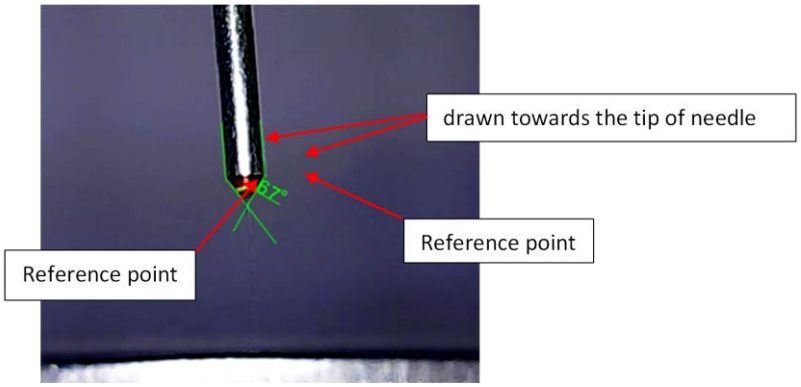

Fig. 3. Positioning of angle that has been measured

A line is drawn approximately on both sides of the needle moving toward the tip of the needle. Then, the end of the line becomes the reference point to draw straight lines along the electrospray Taylor cone. To guarantee accurate measurement of the orientation of each bead, these lines are precisely aligned with its longitudinal axis. Next, an angle measurement tool in AutoCAD is used to figure out the angle between the line drawn along the Taylor cone's as shown in Figure 3. This capability allows you to precisely estimate bead angles, which is critical when analyzing the stability and direction of the electrospray jet.

3. Results

In this part the observation of the electrospray pattern is observed using the microscope camera. And then the picture has been analyzed by using AutoCAD to calculate and identify the angle generated from the Taylor cone. Then the correlation between the changes in the parameter and angle of the jet beat generated will be elaborated here.

3.1 Modes of Electrospray

Figure 4 shows the results observed in the experimental setup. Based on past studies and current observations, it is understood that the electrospray pattern can be categories in 5 modes which are

dripping mode (DM), spindle mode (SM), Taylor cones or cone jet (JB), titled jet (TJ) and flying current (FC). The same kind of results can be observed in past investigations by Kim *et al.,* [18] and Panahi *et al.,* [31]. The dripping mode is shown in Figure 4(a), based on the observation it is understood that the electric current had no effect on the water, and droplets produced with the same diameter as the nozzle due to gravity. Figure 4(b) exemplifies the spindle mode. A motion where the nozzle tip discharges a division of cone and a jet, ultimately permeating into droplets at consistent intervals. The cone from the spindle mode can remain for extended periods, and the jet emitted is rather more pervasive than in cone jet mode. Looking more incisively, the lasting cone formation from the spindle mode at the nozzle's tip insinuates a stable and enduring phase before droplet genesis, in contrast to other modes. This spindle's jet, which is notably much broader than typical cone jets ripples over the ensuing droplets. As anticipated, it leads to a more meticulous and uniform liquid fragmentation.

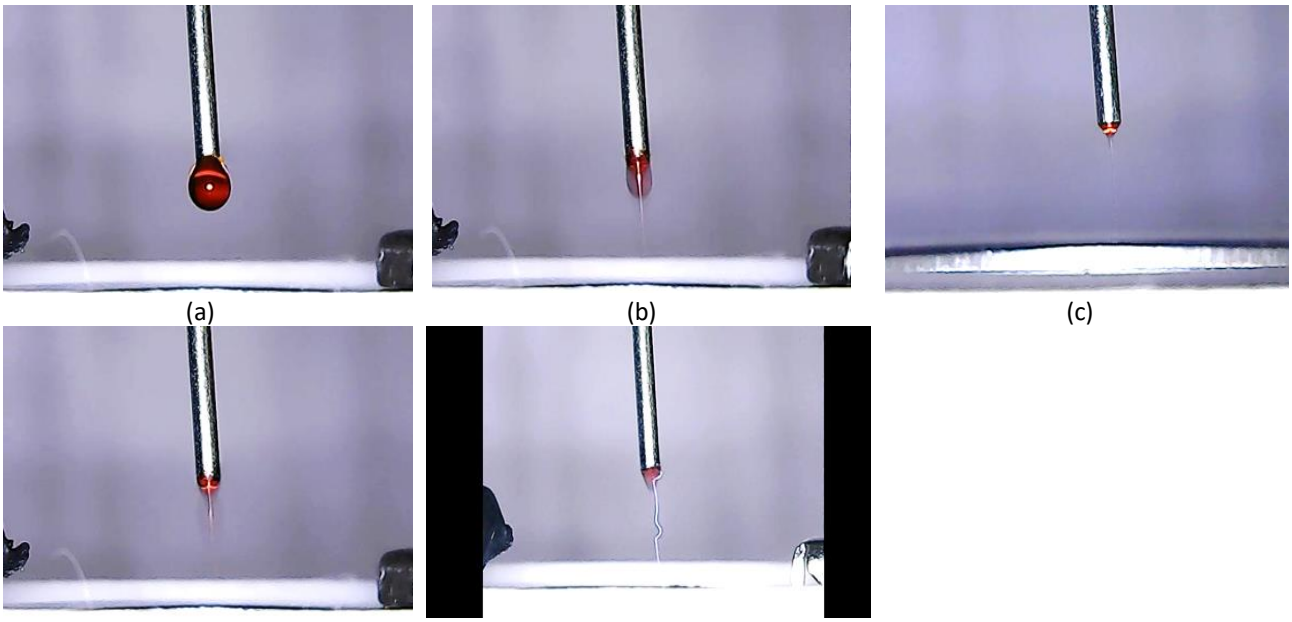

Fig. 4. Modes of electrospray (a) Dripping mode (DM) (b) Spindle Mode (SM) (c) Taylor cone or cone jet (JB) (d) Tilted jet (TJ) (e) Flying current (FC)

Implicitly, this logic results in dribbles of consistent gestation. The Taylor cones mode or similar called cone jet mode exhibited the most stable spray, and the length of the cone increased with the increasing voltage that can be observed on Figure 4(c). In the tilted jet shown in Figure 4(d), the jet at the tip of the cone was tilted to one side during spraying after the cone jet was formed. This occurred because of the influence of the electric field when the jet was broken up due to the surface shear stress from the tip of the cone. Finally, Figure 4(e) shows the development of a flying current in electrospray systems when a specific voltage threshold is reached. The intensity of the electric field near the electrospray emitter's tip, typically a capillary, is directly influenced by the applied voltage and the electrode geometry of the ionization ring. As the applied voltage approaches certain levels the electric field intensity may reach sufficient levels to ionize solvent molecules. This ionization process releases charged particles, thereby generating a flying current. At higher voltages, particularly around 10 kV, the electric field strength may exceed the dielectric breakdown threshold of the surrounding air or solvent vapor. This phenomenon can induce corona discharge, resulting in the emission of ions from the surfaces of the electrodes or the electrospray emitter's tip [42]. These processes collectively contribute to the occurrence of a flying current as charged particles are dispersed into the surrounding environment [43].

Figure 5 shows the multi-jet mode (MT) which are the effects of low and middle flow rates in relations to the voltage applied to the liquid medium [18]. Flow rates exhibit three distinct bands of fluctuation which are low, medium, and high. Each of these bands often achieves certain objectives. For electrospray and similar applications, the low flow rate is typically between 0.01 mL/min and 0.05 mL/min, with a relatively narrow range. The droplets at that location are minuscule, resulting in a heightened level of precision. A middle range of flow rates, ranging from 0.05 to 2.00 mL/min, achieves a harmonious balance between droplet size and flow rate. In this context, consistent operations can achieve efficiency. Industrial applications need a high flow rate, ranging from 2.00 mL/min to 50.00 mL/min. Larger volumes of liquid are necessary for versatile applications such as spraying and coating.

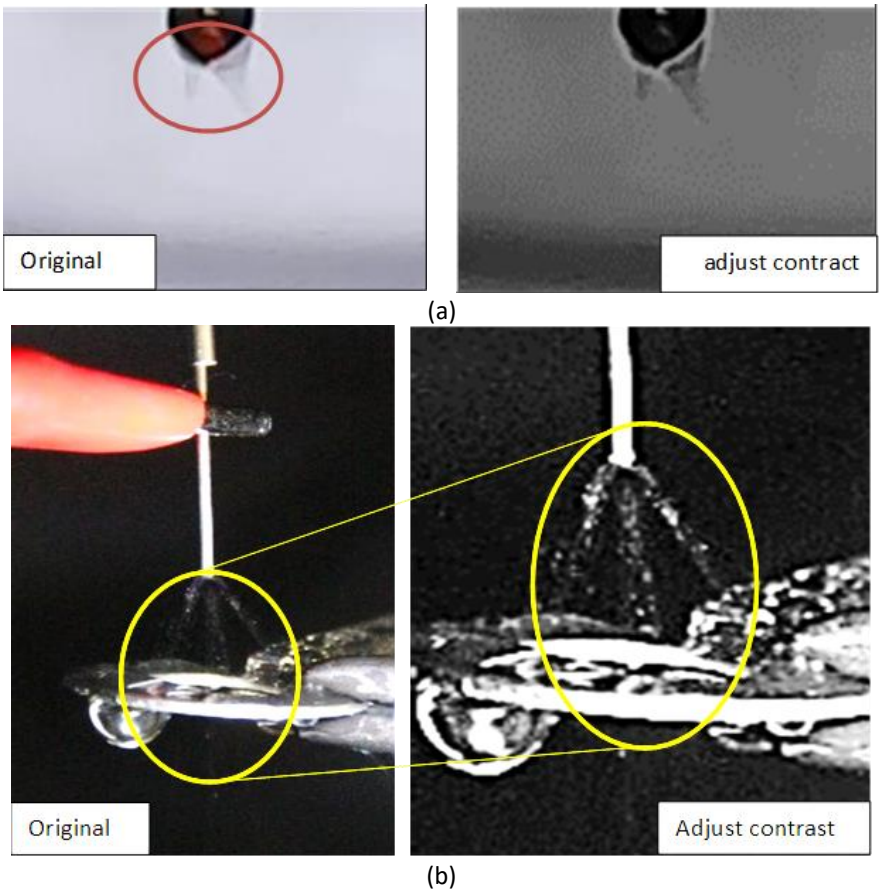

Fig. 5 Difference mode electrospray based on flow rate (a) Multi-jet (MT) (b) Pulsed jet (PT)

Furthermore, the accuracy of the flow rate measurement significantly influences the results. Particularly small, aerosolized particles require a consistent electrospray. MT is an effect that happens when the liquid medium is sprayed in two or three directions as shown in Figure 5(a) and Figure 5(b). As observed in our results, MT occurs when the needle is placed in a position past the IR, or the experimental setup are in the position B. Based on our results as shown in Figure 5(a) and Figure 5(b), in the MT's two and three directions of sprays occur, this kind of effects happen when the flowrates of the liquid medium are set approximately 0.1 mL/min and it's called pulse jet mode (PT). And whenever the flowrates are increased up to approximately 1.0 mL/min, the three directions of spray occur. For both cases of flowrates, the voltage is set constant at 5.5 kV to 6.6 kV. Thus, based on the influence it is safe to state that these two conditions show an effect of manipulating the flow rate of the mediums that influences the Taylor cones formation or characteristics.

The MT represents a significant breakthrough in electrospraying techniques, since it causes the production of a weak cone, which commences the simultaneous growth of numerous jet branches. This phenomenon happens when many jets are created at the same time under high voltage and low flow rate circumstances. The interplay of these factors, namely the applied voltage and flow rate, has a significant impact on the features of the jet generated. It has been discovered that raising the flow rate increases the thickness of the jet, most likely because more solvent is evacuated per unit time. On the other hand, raising the applied voltage lowers the thickness of the jet, which is due to the increased electrostatic force that encourages the jet's spreading and elongation. This delicate interplay between voltage and flow rate demonstrates the complex dynamics that regulate the multi-jet mode in electrosprays, emphasizing their importance in maximizing ionization efficiency and performance in analytical applications.

3.2 Data Analysis

Tables 1 and 2 show the results observed during the experimentation of the electrospray modes respectively for needle in position A and position B. The table tabulated the voltage applied in kV, IDIR, mode of electrospray and angle generated from the cone developed at the tip of the needle. In general, for both cases (position A and position B) the electric current starts to give an effect at the voltage of 4.5 kV applied to the water. The larger the IDIR, the wider the range of voltage can be used to generate the modes of electrospray.

Based on the data tabulated in Tables 1 and 2, the analysis of the electrospray mode and the corresponding voltage and angle variations of the Taylor cone will reveal various patterns and transition. To explain the results, the voltage of the collected data is grouped in a category of low voltage, mid-voltage and high voltage. The low voltage is assumed within the range of 3.0 kV to 4.0 kV, mid-range voltage is within the range of 4.5 kV to 6.0 kV and finally the high voltage is more than 6.0 kV. At the lower voltage 3.0 kV and 3.5 kV, both setup of position A and position B consistently shows the DM regardless the ID of the IR (10.3 mm, 15.3 mm, and 21.2 mm). However, at 4.0 kV, the mode remains predominantly DM, except for setup of position A and the use of 10.3 mm for IDIR where the mode transitions to the SM. As the voltage increases beyond 4.0 kV, more complex behaviors emerge. Regardless the IDIR, and position of the experimental setup, the JB occurs at 4.5 kV, however the TJ, MT and Intermittent JB modes emerge at transition of voltage between mid-range and higher voltages of approximately in the range of 5.5 kV to 6.0 kV, showing a transition toward more dynamic spray modes. In particular, the transition from DM to JB occurs at approximately 4.5 kV for both position A and position B setup, indicating a similar voltage threshold for this transformation. Developing TJ, MT and Intermittent JB modes between 5.5 and 6.0 kV shows another threshold during which electrospray behavior becomes more intermittent and jet-like.

The Intermittent JB (Intermittent Jetting-Breakup) mode in electrospray occurs when the liquid flow from the nozzle or capillary is unstable, fluctuating between jetting and breaking up into droplets. Voltage, speed of flow, and IR influence can all have an impact on this mode. At some voltages, the electric field may be strong enough to start jetting but insufficiently stable to sustain a steady jet, resulting in intermittent jet formation and breakdown. If the fluid's flow rate is inconsistent, it can result in intermittent jetting, with higher flow rates driving the liquid into a continuous jet and lower flow rates splitting it into droplets. Furthermore, the design and direction of the IR can influence jet stability since non-uniform electric fields induced by electrode shape or location result in intermittent jetting. The physical qualities of the liquid, such as its tension on the surface and consistency, also affect jet stability, with higher surface tension leading the jet to break

apart more easily. Capillary instability, caused by the electric field's interaction with the liquid's surface tension, can also cause the jet to oscillate between steady jetting and droplet formation.

Table 1
The data collection is based on spray pattern and angle between the needle and the ionization ring for position A

IDIR (mm)	10.3		15.3		21.2	
Voltage (kV)	Mode	Angle (°)	Mode	Angle (°)	Mode	Angle (°)
3.0	DM	0	DM	0	DM	0
3.5	DM	0	DM	0	DM	0
4.0	SM	0	DM	0	DM	0
4.5	JB	64	JB	38	JB	38
5.0	JB	68	JB	37	JB	61
5.5	Intermittent JB	70	JB	37	JB	61
6.0	TJ	77	Intermittent JB	42	Intermittent JB	65
6.5	FC	0	Spray	42	Intermittent JB	65
7.0			Intermittent JB	43	JB	67
7.5			Intermittent JB	43	JB	71
8.0			Spray	43	Intermittent JB	65
8.5			Intermittent JB	43	Intermittent JB	65
9.0			JB	43	JB	71
9.5			FC	0	JB	71
10.0					FC	0

Table 2
The data collection based on spray pattern and angle due needle passes the ionization ring for position B

IDIR (mm)	10.3		15.3		21.2	
Voltage (kV)	Mode	Angle (°)	Mode	Angle (°)	Mode	Angle (°)
3.0	DM	0	DM	0	DM	0
3.5	DM	0	DM	0	DM	0
4.0	DM	0	DM	0	DM	0
4.5	JB	62	JB	47	DM	0
5.0	JB	84	JB	46	DM	0
5.5	MT	80	MT	38	JB	25
6.0	Intermittent JB	65	JB	50	MT	27
6.5	FC	0	JB	54	MT	27
7.0			JB	54	Intermittent JB	30
7.5			JB	54	JB	31
8.0			JB	54	JB	35
8.5			JB	54	JB	35
9.0			FC	0	JB	35
9.5					JB	35
10.0					JB	35

Subsequently, when a liquid is electrosprayed, the electric field creates a charge on the liquid's surface, forming a Taylor cone and emitting a narrow jet of liquid. The jet's stability is regulated by a balance of electrostatic forces that push the liquid out and surface tension that pulls it back. If this balance is lost, the jet becomes unstable. The electric field may not generate a continuous jet at some voltage levels, resulting in intermittent jetting. If the liquid flow rate does not remain constant, the amount of liquid available to generate the jet changes, resulting in intermittent behavior.

In the provided datasets, intermittent JB appears at different voltages for different IDIRs, at 5.5 kV and 6.0 kV for the 10.3 mm ionization ring, at 6.0 kV, 6.5 kV, and higher voltages for the 15.3 mm ionization ring, and at 6.0 kV for the 21.2 mm ionization ring, indicating that both voltage and

electrode geometry influence this mode. The jet's intermittent behavior is most likely caused by a delicate balance of forces under these conditions, which causes it to develop and dissipate on a frequent basis.

Overall, both setup of position A and position B shows a clear and constant pattern of mode transitions with increasing voltage, revealing an important aspect of the electrospray process. The IDIR influences the angle of the Taylor cone, with bigger IDIR will produces smaller angle. The more consistent angle readings are observed for setup of position B, where the angle of the Taylor cone started to give constant value regardless of the voltage given. Such behavior is not observed in the setup of position A. In summary, increasing voltage consistently results in the shift from DM to more complicated modes such as JB, TJ and MT, with the IDIR having a substantial impact on angle of the Taylor cone. However, for setup in position B, the angle of Taylor cone becomes stable and constant at certain voltage.

3.3 Correlation Between Voltage, and Taylor Cones in Relation to the Parameter Changes

To further understand the characteristics of the electrospray modes, the voltage versus angle of Taylor cone is plotted in Figure 6 and Figure 7 for position A and position B, respectively. In Position A, as shown in Figure 6, the 10.3 mm IDIR exhibits a clear correlation between increasing voltage and spray angle, which ranges from approximately 60° at 4.5 kV to nearly 80° at 9.5 kV. This steady rise implies that wider spray angles, which are a sign of more distributed Taylor cone formations, are encouraged by higher voltages. The 15.3 mm IDIR exhibits a consistent spray angle, with slight variations around 40° up to 10 kV, beginning at roughly 38° at 4.5 kV and reaching about 43° at 5.5 kV. For this IDIR, the relative stability of the spray angle suggests that voltage variations have a less noticeable impact on Taylor cone dispersion. For the 21.2 mm IDIR, the spray angle increases rapidly from about 42° at 4.5 kV to approximately 60° at 5.5 kV, followed by a gradual rise, stabilizing approximately 65-70° between 6 kV and 10 kV. This pattern suggests a strong initial impact of voltage on Taylor cone dispersion, which becomes more stable at higher voltages. The spray angle for the 21.2 mm IDIR rises quickly from around 42° at 4.5 kV to about 60° at 5.5 kV. After that, it rises more gradually and stabilizes at 65–70° between 6 kV and 10 kV. This pattern suggests that voltage initially has a significant effect on Taylor cone dispersion and then stabilizes at higher values.

On the other hand, the 10.3 mm IR in Position B, as seen in Figure 7, exhibits a peak spray angle that rises dramatically from around 65° at 4.5 kV to 85° at 5 kV, then drops to approximately 60° at 6.5 kV before stabilizing up to 10 kV. Triangle symbols indicate a slanted jet phenomenon at 5 kV, which is shown by a dip that follows this peak. This behavior suggests that there is an imbalance in the electrostatic forces influencing the Taylor cone's stability. The spray angle of the 15.3 mm IR is constant, beginning at around 50° at 4.5 kV, gradually falling to about 45° at 5.5 kV, and staying at about 50° until 10 kV. Taylor cone production is constant due to stability, which exhibits low susceptibility to voltage variations. The spray angle for the 21.2 mm IR steadily rises from around 35° at 4.5 kV to roughly 45° at 6 kV before stabilizing at 10 kV. Like Position A, this trend shows steady Taylor cone development as voltage rises. The data points with circles indicate the intermittent spray behavior that happens at specific voltages for the 10.3 mm and 21.2 mm sizes of IDIR. For the 10.3 mm IR, MT behavior was seen at 5 kV and 5.5 kV. This indicates instability in Taylor cone production at these voltages, most likely because of transitional spray regimes.

On overall the results show that the Taylor cone started to develop at the voltage of 4 kV. Increasing the voltage helps in stabilizing the Taylor cone, however after certain value of voltage FC starts to occur and Taylor cone will be destroyed since as a safety measure the current will automatically be cut off. It is understood from those results for both positions of the needle, the

Taylor cone will become constant after certain voltage. And it is safe to state that the position B setup develops a more stable Taylor cone and has wider voltage range as compared to position A.

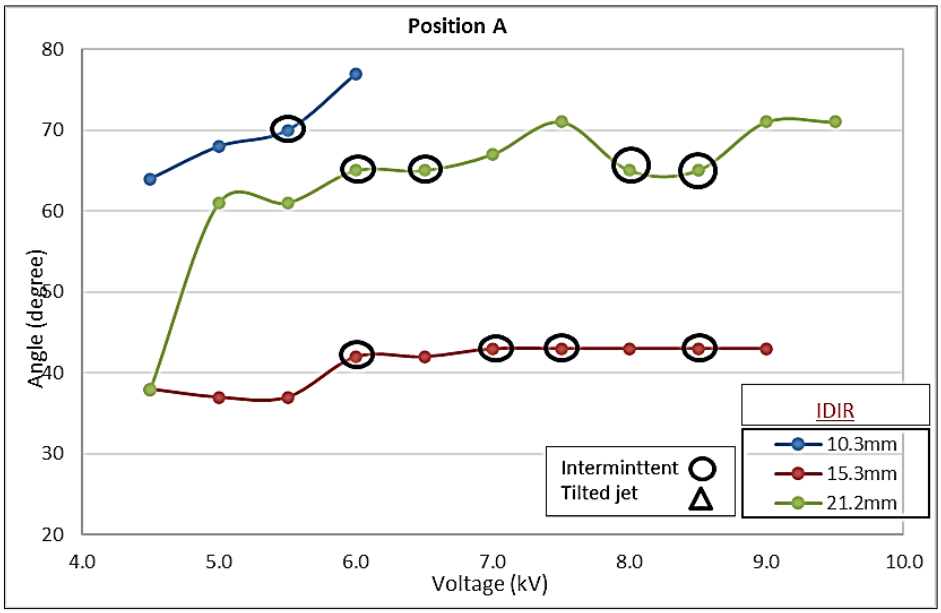

Fig. 6. Analysis of Taylor cone patterns through the ionization ring in position A

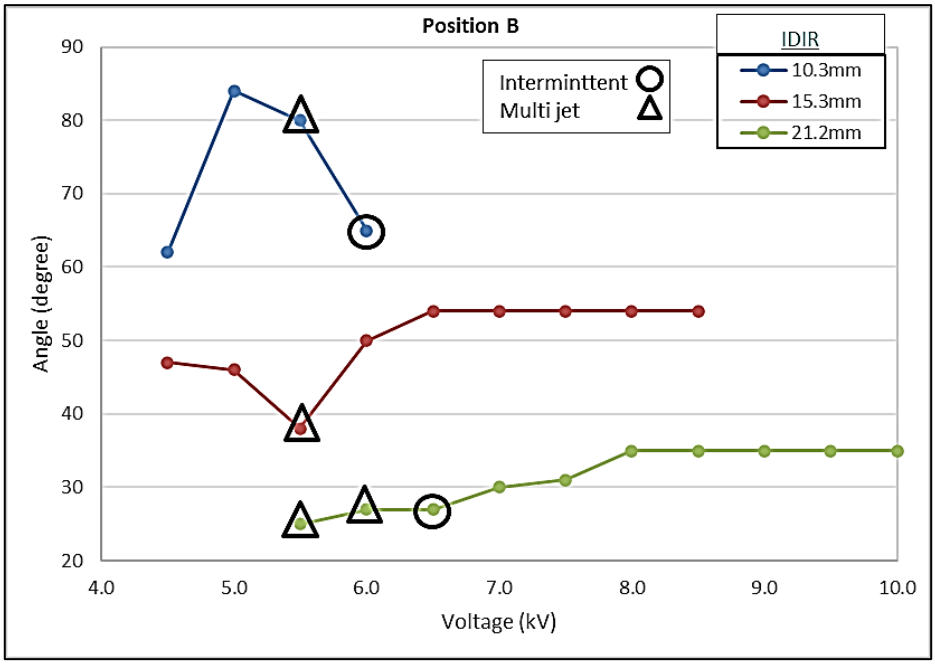

Fig. 7. Analysis of Taylor cone patterns through the ionization ring in position

4. Conclusions

In this study the effects of inner diameter and position of ionization ring were evaluated in relation to the effects of voltage applied and Taylor cone generated. It was found that the Taylor cone starts to develop at 4 kV and depends on the needle position and inner diameter of Ionization Ring (IDIR), flying current start to occurs that cut off the current. Additionally, for IDIR of 15.3 mm and 21.2 mm, a constant angle of Taylor cone starts to develop at certain voltage. It also found that

for position B, the generated Taylor cone is more stable and has a larger voltage range to generate Taylor cone.

Future study should look at extensive quantitative analysis to determine the precise impacts of different voltage and ionization ring parameters on Taylor cone production. Furthermore, it would be advantageous to investigate the long-term stability and consistency of the electrospray process under various operational settings, as well as the effect of diverse liquid sample parameters, such as viscosity and conductivity, on electrospray performance. It is also encouraged to investigate external environmental parameters such as temperature and humidity and how these affect the electrospray process and Taylor cone properties, as well as to use modern imaging techniques for high-resolution, real-time data acquisition.

Acknowledgement
This research work is sponsored by research grant FRGS/1/2022/TK10/UTEM/02/26/F00512. Authors would like to thank Ministry of Higher Education (MOHE) and University Technical Malaysia Melaka (UTeM) for sponsoring this research work.

References

[1] Alfatama, Mulham, Yasser Shahzad, and Hazem Choukaife. "Recent advances of electrospray technique for multiparticulate preparation: Drug delivery applications." *Advances in Colloid and Interface Science* (2024): 103098. https://doi.org/10.1016/j.cis.2024.103098

[2] Yang, Dongmei, Bo Wang, Yuchuan Wang, Aiping Liu, Jiguang Liu, and Min Zhang. "Microbial inactivation of pressure spray combined with high-voltage electrospray and its application in honey raspberry juice." *International Journal of Food Microbiology* 413 (2024): 110602. https://doi.org/10.1016/j.ijfoodmicro.2024.110602

[3] Sereshkeh, S. Rahman Pejman, Bryan Llumiquinga, Sriya Bapatla, Michael J. Grzenda, David Specca, Arend-Jan Both, and Jonathan P. Singer. "Staticaponics: Electrospray delivery of nutrients and water to the plant root zone." *Journal of Electrostatics* 128 (2024): 103902. https://doi.org/10.1016/j.elstat.2024.103902

[4] Jumaidin, Ridhwan, Mohd Sapuan Salit, Mohamed Saiful Firdaus, Ahmad Fuad Ab Ghani, Mohd Yuhazri Yaakob, Nazri Huzaimi Zakaria, Fudhail Abdul Munir, Azrul Abidin Zakaria, and Norhisyam Jenal. "Effect of agar on dynamic mechanical properties of thermoplastic sugar palm starch: Thermal behavior." *Journal of Advanced Research in Fluid Mechanics and Thermal Sciences* 47, no. 1 (2018): 89-96.

[5] Saleman, Abdul Rafeq bin, Hari Krishna Chilukoti, Gota Kikugawa, and Taku Ohara. "A molecular dynamics study on the thermal rectification effect at the solid–liquid interfaces between the face-centred cubic (FCC) of gold (Au) with the surfaces of (100),(110) and (111) crystal planes facing the liquid methane (CH4)." *Molecular Simulation* 45, no. 1 (2019): 68-79. https://doi.org/10.1080/08927022.2018.1535177

[6] Lambropoulos, Nicholas. "High Performance liquid chromatography and electrospray mass spectrometry of zinc dithiophosphates as Lubricating Oil Additives." PhD diss., La Trobe, 1995.

[7] Wang, Shi, Arian Yazdkhsti, As' ad Alizadeh, Ali Basem, Dheyaa J. Jasim, Ameer H. Al-Rubaye, Soheil Salahshour, and Davood Toghraie. "Calculating minimum droplet diameter in dripping, spindle, and cone-jet modes based on experimental data in the electrospray process." *Experimental Thermal and Fluid Science* (2024): 111154. https://doi.org/10.1016/j.expthermflusci.2024.111154

[8] Zhang, Chen, Xiao Wang, Meng Xiao, Jiaqi Ma, Yan Qu, Liang Zou, and Jinming Zhang. "Nano-in-micro alginate/chitosan hydrogel via electrospray technology for orally curcumin delivery to effectively alleviate ulcerative colitis." *Materials & Design* 221 (2022): 110894. https://doi.org/10.1016/j.matdes.2022.110894

[9] Yang, Shiqi, Zhentao Wang, Qian Kong, Bin Li, and Junfeng Wang. "Visualization on electrified micro-jet instability from Taylor cone in electrohydrodynamic atomization." *Chinese Journal of Chemical Engineering* 44 (2022): 456-465. https://doi.org/10.1016/j.cjche.2021.03.005

[10] Jahan, Sultana, M. Ferdows, M. D. Shamshuddin, and Khairy Zaimi. "Effects of solar radiation and viscous dissipation on mixed convective non-isothermal hybrid nanofluid over moving thin needle." *Journal of Advanced Research in Micro and Nano Engineering* 3, no. 1 (2021): 1-11.

[11] Wang, Zhentao, Yonghui Zhang, Tianyu Guo, Zhonghui Zhu, Xiaoying Wang, and Jianlong Wen. "Experimental study on size and velocity of charged droplets." *Procedia Engineering* 126 (2015): 522-526. https://doi.org/10.1016/j.proeng.2015.11.295

[12] Bošković, Stefan, and Branko Bugarski. "Review of electrospray observations and theory." *Journal of Engineering & Procesing Management* 10, no. 2 (2018): 41-53. https://doi.org/10.7251/JEPM181002041B
[13] Yeo, Leslie Y., Zachary Gagnon, and Hsueh-Chia Chang. "AC electrospray biomaterials synthesis." *Biomaterials* 26, no. 31 (2005): 6122-6128. https://doi.org/10.1016/j.biomaterials.2005.03.033
[14] Ondimu, O. M., V. A. Ganesan, M. J. Gatari, J. C. M. Marijnissen, and L. L. F. Agostinho. "Modeling simple-jet mode electrohydrodynamic-atomization droplets' trajectories and spray pattern for a single nozzle system." *Journal of Electrostatics* 89 (2017): 77-87. https://doi.org/10.1016/j.elstat.2017.08.001
[15] Wu, Hao, Niels Mendel, Stijn van Der Ham, Lingling Shui, Guofu Zhou, and Frieder Mugele. "Charge trapping-based electricity generator (CTEG): An ultrarobust and high efficiency nanogenerator for energy harvesting from water droplets." *Advanced materials* 32, no. 33 (2020): 2001699. https://doi.org/10.1002/adma.202001699
[16] Namoos, Haedir Abd AlRazak, and Abeer Majeed Jasim. "The analytical improvement of q-homotopy analysis method for magneto-hydrodynamic (MHD) Jeffrey Hamel nanofluid flow." *Journal of Advanced Research in Fluid Mechanics and Thermal Sciences* 119, no. 2 (2024): 32-55. https://doi.org/10.37934/arfmts.119.2.3255
[17] Zhang, Jinrui, Guobiao Cai, Xuhui Liu, Bijiao He, and Weizong Wang. "Molecular dynamics simulation of ionic liquid electrospray: Revealing the effects of interaction potential models." *Acta Astronautica* 179 (2021): 581-593. https://doi.org/10.1016/j.actaastro.2020.11.018
[18] Kim, Ji Yeop, Sang Ji Lee, and Jung Goo Hong. "Spray mode and monodisperse droplet properties of an electrospray." *ACS omega* 7, no. 32 (2022): 28667-28674. https://doi.org/10.1021/acsomega.2c04002
[19] Nashee, Sarah Rabee, and Haiyder Minin Hmood. "Numerical study of heat transfer and fluid flow over circular cylinders in 2D cross flow." *Journal of Advanced Research in Applied Sciences and Engineering Technology* 30, no. 2 (2023): 216-224. https://doi.org/10.37934/araset.30.2.216224
[20] Xian, Hong Wei, Rahman Saidur, Nor Azwadi Che Sidik, and Yutaka Asako. "Viscosity of CuO nanofluid due to nanoparticles size and concentration." *Journal of Advanced Research in Applied Sciences and Engineering Technology* 28, no. 1 (2022): 161-167. https://doi.org/10.37934/araset.28.1.161167
[21] Zhao, Kun, Wei Wang, Yaoyao Yang, Ke Wang, and Deng-Guang Yu. "From Taylor cone to solid nanofiber in tri-axial electrospinning: Size relationships." *Results in Physics* 15 (2019): 102770. https://doi.org/10.1016/j.rinp.2019.102770
[22] Naderi, Pejman, Mehrzad Shams, and Hojat Ghassemi. "Investigation on the onset voltage and stability island of electrospray in the cone-jet mode using curved counter electrode." *Journal of Electrostatics* 98 (2019): 1-10. https://doi.org/10.1016/j.elstat.2019.01.004
[23] Wang, Yingxi, Wenluan Zhang, Qiangqiang Sun, Shiji Lin, Sheng Sun, and Xu Deng. "Facile strategy to generate charged droplets with desired polarities." *ACS omega* 5, no. 41 (2020): 26908-26913. https://doi.org/10.1021/acsomega.0c04140
[24] Camelot, D. M. A., R. P. A. Hartman, J. C. M. Marijnissen, B. Scarlett, and D. Brunner. "Experimental study of the jet break up for ehda of liquids in the cone-jet mode." *Journal of Aerosol Science* 30, no. 7 (1999): 976-977. https://doi.org/10.1016/S0021-8502(98)00060-3
[25] Crotti, Sara, Roberta Seraglia, and Pietro Traldi. "Some thoughts on electrospray ionization mechanisms." *European journal of mass spectrometry* 17, no. 2 (2011): 85-99. https://doi.org/10.1255/ejms.1129
[26] Hartman, Ruppert PA, D. J. Brunner, D. M. A. Camelot, Jan CM Marijnissen, and Brian Scarlett. "Jet break-up in electrohydrodynamic atomization in the cone-jet mode." *Journal of aerosol science* 31, no. 1 (2000): 65-95. https://doi.org/10.1016/S0021-8502(99)00034-8
[27] Wang, Fanjin, Moe Elbadawi, Scheilly Liu Tsilova, Simon Gaisford, Abdul W. Basit, and Maryam Parhizkar. "Machine learning predicts electrospray particle size." *Materials & Design* 219 (2022): 110735. https://doi.org/10.1016/j.matdes.2022.110735
[28] Hartman, R. P. A., D. J. Brunner, D. M. A. Camelot, J. C. M. Marijnissen, and B. Scarlett. "Electrohydrodynamic atomization in the cone–jet mode physical modeling of the liquid cone and jet." *Journal of Aerosol science* 30, no. 7 (1999): 823-849. https://doi.org/10.1016/S0021-8502(99)00033-6
[29] Jweeg, Mohsen, Emad Qasem Hussein, Farhan Lafta Rashid, and Ali Basem. "Investigation of two-way fluid-structure interaction of blood flow at different temperature using CFD." *Journal of Advanced Research in Applied Sciences and Engineering Technology* 36, no. 2 (2023): 120-130. https://doi.org/10.37934/araset.36.2.120130
[30] Bruins, Andries P. "Mechanistic aspects of electrospray ionization." *Journal of Chromatography A* 794, no. 1-2 (1998): 345-357. https://doi.org/10.1016/S0021-9673(97)01110-2
[31] Panahi, Amirreza, Ahmad Reza Pishevar, and Mohammad Reza Tavakoli. "Experimental investigation of electrohydrodynamic modes in electrospraying of viscoelastic polymeric solutions." *Physics of Fluids* 32, no. 1 (2020). https://doi.org/10.1063/1.5132556
[32] Ganán-Calvo, Alfonso M., José M. López-Herrera, Miguel A. Herrada, Antonio Ramos, and José M. Montanero. "Review on the physics of electrospray: From electrokinetics to the operating conditions of single and coaxial Taylor

cone-jets, and AC electrospray." *Journal of Aerosol Science* 125 (2018): 32-56. https://doi.org/10.1016/j.jaerosci.2018.05.002

[33] Rovelli, Grazia, Michael I. Jacobs, Megan D. Willis, Rebecca J. Rapf, Alexander M. Prophet, and Kevin R. Wilson. "A critical analysis of electrospray techniques for the determination of accelerated rates and mechanisms of chemical reactions in droplets." *Chemical science* 11, no. 48 (2020): 13026-13043. https://doi.org/10.1039/D0SC04611F

[34] Thuppul, Anirudh, Peter L. Wright, Adam L. Collins, John K. Ziemer, and Richard E. Wirz. "Lifetime considerations for electrospray thrusters." *Aerospace* 7, no. 8 (2020): 108. https://doi.org/10.3390/aerospace7080108

[35] Kang, Zhuang, Zhiwei Shi, Jiahao Ye, Xinghua Tian, Zhixin Huang, Hao Wang, Depeng Wei, Qingguo Peng, and Yaojie Tu. "A review of micro power system and micro combustion: present situation, techniques and prospects." *Energies* 16, no. 7 (2023): 3201. https://doi.org/10.3390/en16073201

[36] Yamaguchi, Kentaro. "Cold-spray ionization mass spectrometry: Applications in structural coordination chemistry." *Mass Spectrometry* 2, no. Special_Issue (2013): S0012-S0012. https://doi.org/10.5702/massspectrometry.S0012

[37] Huang, Kai-Hung, Jyotirmoy Ghosh, Shiqing Xu, and R. Graham Cooks. "Late-stage functionalization and characterization of drugs by high-throughput desorption electrospray ionization mass spectrometry." *ChemPlusChem* 87, no. 1 (2022): e202100449. https://doi.org/10.1002/cplu.202100449

[38] Ouyang, Zheng, and R. Graham Cooks. "Miniature mass spectrometers." *Annual Review of Analytical Chemistry* 2, no. 1 (2009): 187-214. https://doi.org/10.1146/annurev-anchem-060908-155229

[39] Zhong, Xiaoqin, Liang Qiao, Géraldine Stauffer, Baohong Liu, and Hubert H. Girault. "On-chip spyhole nanoelectrospray ionization mass spectrometry for sensitive biomarker detection in small volumes." *Journal of The American Society for Mass Spectrometry* 29, no. 7 (2018): 1538-1545. https://doi.org/10.1007/s13361-018-1937-7

[40] Magnusson, Jared M., Adam L. Collins, and Richard E. Wirz. "Polyatomic ion-induced electron emission (IIEE) in electrospray thrusters." *Aerospace* 7, no. 11 (2020): 153. https://doi.org/10.3390/aerospace7110153

[41] Jiang, Jiaxin, Zunxu Qian, Xiang Wang, Huatan Chen, Guoyi Kang, Yifang Liu, Gaofeng Zheng, and Wenwang Li. "Numerical simulation of motion and distribution characteristics for electrospray droplets." *Micromachines* 14, no. 2 (2023): 396. https://doi.org/10.3390/mi14020396

[42] Pongrác, Branislav, Hyun-Ha Kim, Nobuaki Negishi, and Zdenko Machala. "Influence of water conductivity on particular electrospray modes with dc corona discharge—optical visualization approach." *The European Physical Journal D* 68 (2014): 1-7. https://doi.org/10.1140/epjd/e2014-50052-4

[43] Ganán-Calvo, Alfonso M., José M. López-Herrera, Miguel A. Herrada, Antonio Ramos, and José M. Montanero. "Review on the physics of electrospray: from electrokinetics to the operating conditions of single and coaxial Taylor cone-jets, and AC electrospray." *Journal of Aerosol Science* 125 (2018): 32-56. https://doi.org/10.1016/j.jaerosci.2018.05.002